

# Effect of injection molding parameters on nanofillers dispersion in masterbatch based PP-clay nanocomposites

J. J. Rajesh<sup>1,2</sup>, J. Soulestin<sup>1,2\*</sup>, M. F. Lacrampe<sup>1,2</sup>, P. Krawczak<sup>1,2</sup>

<sup>1</sup>Université Lille Nord de France, F-59000 Lille, France

<sup>2</sup>Ecole des Mines de Douai, Department of Polymers and Composites Technology & Mechanical Engineering, 941 Rue Charles Bourseul, BP 10838, F-59508, Douai, France

Received 15 June 2011; accepted in revised form 5 October 2011

**Abstract.** The effect of injection molding parameters (screw rotational speed, back pressure, injection flow rate and holding pressure) on the nanofiller dispersion of melt-mixed PP/clay nanocomposites was investigated. The nanocomposites containing 4 wt% clay were obtained by dilution of a PP/clay masterbatch into a PP matrix. The evaluation of the dispersion degree was obtained from dynamic rheological measurements. The storage modulus and complex viscosity exhibit significant dependence on the injection molding parameters. PP/clay nanocomposite molded using more severe injection parameters (high shear and long residence time) displays the highest storage modulus and complex viscosity, which illustrates the improved dispersion of clay platelets. This better dispersion leads to better mechanical properties particularly higher Young modulus, tensile strength and unnotched impact strength. A Taguchi analysis was used to identify the influence of individual process parameters. The major individual parameter is the injection flow rate, whose increase improves nanoclay dispersion. The combination of high back pressure and high screw rotational speed is also necessary to optimize the dispersion of clay nanoplatelets.

**Keywords:** nanocomposites, masterbatch, polypropylene, montmorillonite, rheology

## 1. Introduction

Polymer layered silicate (PLS) nanocomposites are materials in which the reinforcing elements (called nanofillers) are nano-sized at least in one direction leading to very high aspect ratio (length/thickness >100), surface area (100–1000 m<sup>2</sup>/g), and surface area to volume ratio [1–2]. The interfacial effects are therefore predominant in that case compared with the conventional reinforcements like talc or glass fibers even at very low filler loading level (around 5 wt%). Proper dispersion of nanofillers is a key issue, and as soon as it is achieved, is reflected in superior specific mechanical, thermal, flame retardancy and barrier properties [1–2]. The most commonly developed polymer nanocomposites are based on clay silicate layered nanoplatelets and montmo-

rillonite is the most widely used among them due to its natural abundance and high aspect ratio. The extent of property improvement mainly depends on the dispersion and/or exfoliation of clay nanoplatelets. The exfoliation of clay platelets is an uphill task, particularly in non-polar polymer like polypropylene (PP) because of the unfavorable enthalpic interaction with the highly hydrophilic clay, which prohibits the diffusion of polymer molecules into the intergallery space. Even if attempts have been made to use pristine (unmodified) clay [3–6], modification of clay with organic agents and addition of compatibilizers such as maleic anhydride (MA) are common solutions used to improve the interaction between PP and clay nanoplatelets. Thereby improved dispersion and thus mechanical properties may be

\*Corresponding author, e-mail: [jeremie.soulestin@mines-douai.fr](mailto:jeremie.soulestin@mines-douai.fr)  
© BME-PT

achieved [7–14] even if full exfoliation cannot be obtained in PP matrices due to the huge polarity difference between the matrix and the clay [15, 16].

The most popular manufacturing process to produce in an economically viable way very complex shape thermoplastic parts for various industrial applications in a single and rapid automatic step (mass production) is injection molding. However, various parameters viz. screw rotation speed, back pressure, injection flow rate, mold temperature, melt temperature, holding pressure, etc., are likely to affect the properties of the injection molded products. The influence of the above-mentioned parameters on mechanical properties of PP was studied extensively [17–19]. However, the literature available on the influence of these parameters on the dispersion of the nanoplatelets in the clay-based nanocomposites is still limited. Authors mainly focused on extrusion process [20–25].

Besides, direct processing (i.e. addition of the nanofillers directly into the host polymer matrix so as to reach the targeted particle weight content) was generally used in the above-mentioned studies. However, masterbatch-based nanocomposites processing (i.e. dilution in a host thermoplastic of a masterbatch highly concentrated in nanofillers) is usually preferred by plastics converters as it avoids direct handling of health hazardous and environmentally unfriendly nanomaterials in industrial production workshops. Nevertheless, the influence of the masterbatch-based processing conditions on the nanofiller dispersion in polymer nanocomposites is sparsely reported in the literature [25–29].

It is therefore worth clarifying the relationship between various injection-molding conditions and the dispersion of clay nanoplatelets in the case of PP nanocomposites obtained by melt-mixing from a PP/clay masterbatch. The influence of injection flow rate, holding pressure, back pressure and screw rotation speed will be investigated in particular in this study, the nanoclay dispersion being assessed using dynamic rheological measurements.

## 2. Background on assessment of nanofiller dispersion by dynamic rheological measurements

The main issue to solve is to get a representative evaluation of the dispersion degree at the macroscopic scale. Transmission electron microscopy and

X-ray diffraction are widely used but provide qualitative assessment only. Alternatively, dynamic rheology may provide a semi-quantitative evaluation of the clay nanoplatelets dispersion degree as the reduction of the filler size down to nanometric scale substantially modifies the viscoelastic properties of filled polymers [30–33].

Actually, it is well admitted that the exfoliated and/or disordered intercalated silicate layers form a network type structure rendering the system highly elastic as revealed by the appearance of a secondary plateau for the dynamic storage modulus ( $G'$ ) in the low frequency regime. This gradual change of the behavior from liquid-like to solid-like is mainly correlated to the extent of dispersion and distribution of the clay platelets that form a three-dimensional percolating network. The tendency of formation of this mesoscopic structure gradually increases with increasing degree of dispersion of the silicate layers in the polymer matrix. The existence of the solid-like rheological behavior of the polymer/clay nanocomposites is attributed to the frictional interactions between the highly anisotropic silicate layers. They become particularly significant when percolation (defined as the formation of a long range connectivity) is obtained leading to a frequency independent behavior at the lower frequencies.

Hoffmann *et al.* [34] confirmed that the higher storage moduli ( $G'$ ) and the lower terminal slope in  $G'$  vs frequency ( $\omega$ ) plot illustrated the profound interaction between the silicate platelets and their trend to form a three dimensional superstructure. According to Chow *et al.* [35], the stability of the clay dispersion can be related to the terminal slope, i.e. the higher the slope the less stable the clay dispersion. Moreover, the appearance of a stronger shear thinning effect and higher complex viscosity ( $|\eta^*|$ ) in the lower frequency region indicates a strong intercalation and/or exfoliation process of clay platelets. According to these authors, if the clay layers are well separated from each other (i.e. at exfoliated stage), then shear thinning is more likely to occur than in the case of intercalated composites. Also, the frictional and electrostatic interactions between the many dispersed clay platelets can lead to higher complex viscosity value. Wang *et al.* [36] also discussed this issue. The silicate sheets have positively charged edges and negatively charged faces. This electrostatic interaction between the exfoliated clay

platelets leads to strong filler-filler interaction between the clay platelets. The closer vicinity of these clay platelets, probably due to the larger number density and the electrostatic interaction between them, is responsible for higher complex viscosity since the oriented clay platelets under shear field can recover quickly after shear cessation. Galgali *et al.* [8] suggested that the dramatic decrease in creep compliance of compatibilized PP-clay nanocomposites could be due to the frictional interaction between the clay platelets. Therefore larger shear force is required to overcome this frictional interaction between the clay platelets leading to higher complex viscosity value.

Finally, all the authors agree about the correlation between the rheological properties of the nanocomposites at low frequency and the nanofiller dispersion degree. Thus, the comparison of the rheological properties at low frequency of different nanocomposites obtained using various injection molding conditions may allow assessing the influence of each injection molding parameter on the dispersion degree of the clay nanoplatelets.

### 3. Experimental

The materials studied were 4 wt% organoclay filled PP nanocomposites (NC) prepared by diluting a masterbatch containing 40 wt% clay (Nanoblend 1001, PolyOne, USA) with PP homopolymer with a MFI of 12 g/10 min (B10FB, PolyChim, France) by melt blending technique using a twin screw extruder (BC 45, Clextral, France) with length/diameter ratio  $L/D = 28$ . The compounding was carried out using a rotation speed of 70 rpm at a flow rate of 9 kg/h. The barrel and die temperature settings ranged from 200 to 220°C. In these conditions the residence time was about 5 min. The neat PP and extruded PP nanocomposites were injection-molded using a 800 kN clamping force injection molding machine (KM80, Krauss Maffei, Germany). The geometry of the injection-molded samples was a 2 mm thick box with a U shape (Figure 1) so as to roughly reproduce the geometry of many industrial parts (boxes, bumper,

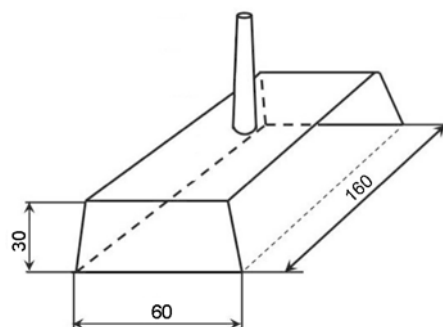


**Figure 1.** Typical part manufactured by injection moulding

dash board insert ...). The mould cavity was fed by a sprue gate. The set-up injection molding conditions (L at low level and H at high level) are compiled in Table 1. The parameters levels were chosen considering the capacity of the injection-molding machine. Preliminary tests were carried out with the studied materials to determine the possible range of parameters (processing window). For instance, the boundaries of holding pressure are the maximum holding pressure reachable by the injection molding machine and the minimum pressure giving a part of good quality.

The designation of the various samples obtained that way is the following: PP-H and NC-H, respectively, for the PP and PP nanocomposites which were injection-molded with all set-up parameters at high levels; PP-L and NC-L, respectively, for the PP and PP nanocomposites which were injection-molded with all set-up parameters at low levels. The influence of individual injection molding parameters on the nanoclay dispersion was studied using a L16 ( $2^{15}$ ) orthogonal array design of experiment (DOE) based on the Taguchi method [37]. The DOE was based on four factors (injection flow rate (Q), holding pressure (HP), back pressure (BP), screw rotation speed (SS)) and two interactions between factors (injection flow rate/holding pressure and screw rotation speed/back pressure). The others processing parameters (holding time, cooling time...) were kept constant. The designation of the nanocomposites samples used for Taguchi analysis is NC-X where X denotes the trial number. Table 2

**Table 1.** Factors (injection molding parameters) and levels selected in the DOE

	Factors				
	Assigned test level	Injection flow rate (Q) [cm <sup>3</sup> /s]	Holding pressure (HP) [bar]	Back pressure (BP) [bar]	Screw speed (SS) [rpm]
Assigned set-up level	High level (H)	50	350	65	90
	Low level (L)	25	250	35	50

**Table 2.** L16 ( $2^{15}$ ) orthogonal array used for the Taguchi DOE

Trial #	Injection flow rate (Q)	Holding pressure (HP)	Back pressure (BP)	Screw rotation speed (SS)
NC-1 (NC-H)	High	High	High	High
NC-2	Low	High	High	High
NC-3	High	Low	High	High
NC-4	High	High	Low	High
NC-5	High	High	High	Low
NC-6	High	High	Low	Low
NC-7	High	Low	High	Low
NC-8	High	Low	Low	High
NC-9	Low	High	High	Low
NC-10	Low	High	Low	High
NC-11	Low	Low	High	High
NC-12	Low	Low	Low	High
NC-13	Low	Low	High	Low
NC-14	Low	High	Low	Low
NC-15	High	Low	Low	Low
NC-16 (NC-L)	Low	Low	Low	Low

gathers the injection-molding parameters of the nanocomposites samples used for the Taguchi analysis.

The dynamic rheological tests were carried out on samples cut from the edge of the U-shaped injection-molded parts using a rotational rheometer (ARES, Rheometric Scientific, USA) in dynamic frequency sweep mode starting from 0.1 to 100 rad/s at 170°C under air atmosphere. The cone and plate configuration with a cone angle of 0.1 rad was used. All the tests were performed at 10% fixed strain rate in the linear viscoelastic domain. PP nanocomposites have a linear viscoelastic behavior until a strain amplitude of about 30%. Storage modulus ( $G'$ ) and complex viscosity ( $|\eta^*|$ ) were calculated from the tests with data collected at ten points per decade.

Mechanical properties of all compounded materials were determined on standard injection-molded test specimens. Young modulus and elongation at break of the molded dog bone shaped test specimens were measured using a tensile machine (Instron 1185, USA) at a crosshead rate of 20 mm/min at 25°C according to ISO 527 standard. Charpy notched and un-notched impact tests were carried out as per ISO 179-1 standard at 25°C using an impact pendulum (Zwick, Germany). All the reported values were calculated as average over five specimens for each composition.

Morphological analysis was performed on cryofactured surfaces of nanocomposites. A thin layer of carbon was sputter deposited onto the sample. Imaging of the nanocomposite was carried out under high vacuum with an Scanning Electron Microscope (S-4300SE/N, Hitachi, Japan) operating at 5 kV.

Structure of the nanocomposites was evaluated by Transmission Electron Microscopy (TEM) on injection-molded samples. Ultrathin sections were cut at ambient temperature with a microtome (Leica Reichert FCS) and collected on a 300 mesh copper grid before observation by TEM microscope (Leo 922).

## 4. Results and discussion

### 4.1. Effect of processing conditions on nanofiller dispersion

Rheological measurements were used to evaluate the dispersion of the clay nanoplatelets for nanocomposites (NC-L and NC-H) obtained by injection molding with different processing parameters. For comparison purpose the neat PP (PP-L and PP-H) was injection molded in the same conditions. Compared to PP-L and NC-L, the nanocomposite NC-H and the PP-H were injection molded with a higher injection flow rate, holding pressure, back pressure and rotational speed so as to increase the dispersion of the clay platelets.

Figures 2 and 3 show the storage modulus ( $G'$ ) and complex viscosity ( $|\eta^*|$ ) as a function of frequency ( $\omega$ ) respectively. The different processing parameters have no significant effect on the rheological

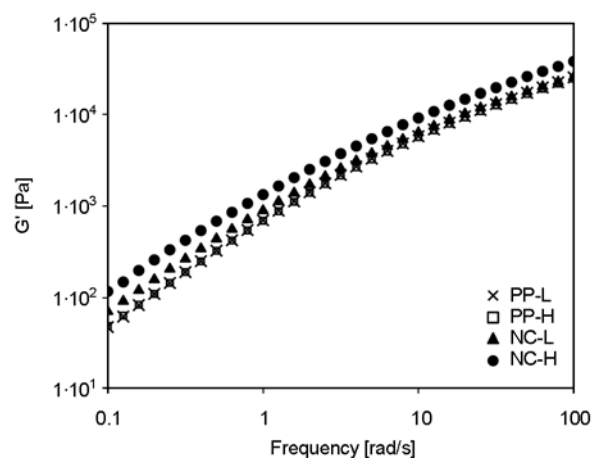


**Figure 2.** Storage modulus ( $G'$ ) as a function of frequency for PP and PP nanocomposites injection molded with all process parameters set-up at low (PP-L, NC-L) level and high (PP-H, NC-H) level

behavior of the polymer matrix, the  $G'$  and  $|\eta^*|$  curves being similar for both PP samples (PP-L and PP-H).  $G'$  at low frequency is higher upon addition of clay into PP. Moreover, the rheological properties are modified depending on injection molding parameters. The storage modulus  $G'$  of the NC-H nanocomposite is higher than the one of the NC-L nanocomposite. As no significant effect of the injection molding parameters is noticed for neat PP, this difference may be ascribed to the improved dispersion of nanoclay when injection flow rate, holding pressure, back pressure and screw rotational speed increase.

Both nanocomposites NC-L and NC-H show no percolation as  $G'$  is frequency dependent even at low frequency (Figure 2). This might be explained by the limited dispersion degree due to unfavorable interaction between PP and clay nanoplatelets and by the low clay content (4% wt), whereas the percolation is generally observed at higher clay concentration [8]. Moreover, this tends to evidence that exfoliation does not occur during injection molding leading to intercalated nanocomposites with a dispersion degree insufficient to achieve a percolation effect. However, during the injection molding process of NC-H nanocomposites, due to better plasticating and/or more severe shearing conditions, the size of the clay tactoids is reduced and the aspect ratio increases. This issue will be discussed later on the basis of microstructural characterization.

The evolution of the complex viscosity  $|\eta^*|$  of both PP references (PP-L and PP-H) is quite similar at all frequencies (Figure 3). In the case of nanocompos-

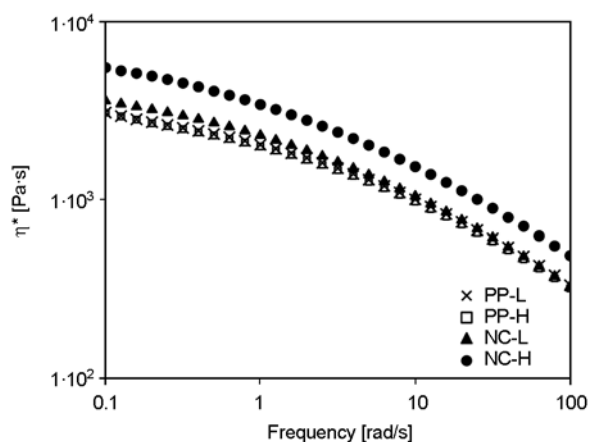


**Figure 3.** Complex viscosity ( $|\eta^*|$ ) as a function of frequency for PP and PP nanocomposites injection molded with all process parameters set-up at low (PP-L, NC-L) level and high (PP-H, NC-H) level

**Table 3.** Terminal slope, storage modulus  $G'$ , shear thinning coefficient  $n$  and complex viscosity  $|\eta^*|$  at 0.1 rad/s of PP and PP/clay nanocomposites

Material	Terminal slope	Storage modulus, $G'$ [Pa]	Shear thinning coefficient, $n$	Complex viscosity, $ \eta^* $ [Pa·s]
PP-L	1.23	48	-0.14	3110
PP-H	1.21	49	-0.15	3104
NC-L	1.00	71	-0.26	3620
NC-H	0.98	107	-0.28	5270

ites (NC-L and NC-H), the viscosities are higher deviating from the behavior of neat PP. The viscosity is also clearly higher for NC-H nanocomposite compared to NC-L nanocomposite confirming the better dispersion obtained in this latter case.

In order to quantitatively assess the clay platelets dispersion in the PP matrix, the storage modulus  $G'$ , complex viscosity  $|\eta^*|$ , terminal slope and shear thinning coefficient  $n$  values of PP and its nanocomposites at 0.1 rad/s are compiled in Table 3. The terminal slope is defined as the slope of the  $G'$  vs frequency ( $\omega$ ) curve in the low frequency region (below 100 rad/s). The shear thinning coefficient is defined as the  $n$  exponent of the power law fitting the complex viscosity vs frequency ( $\omega$ ) curves. At low frequency (0.1 rad/s), the storage modulus and complex viscosity are higher for NC-H than for NC-L nanocomposites. This could be explained as follows. NC-L nanocomposite being molded at lower injection flow rate (meaning lower shear induced during injection step), larger particles are present. The number density of clay platelets and tactoids is therefore lower and might be less than the critical level required to significantly modify the rheological behavior in the low frequency region. Micrographs of cryo-fractured surfaces indicate a number of clay platelets lower for NC-L (Figure 4a) than for NC-H (Figure 5a). Lower number of silicate particles coupled with poor affinity with the apolar PP matrix leads to slightly lower storage modulus and complex viscosity values for NC-L compared to NC-H. Lots of voids or micro-cracks on the surface confirm the poor filler-matrix bonding in both NC-L and NC-H. The other important parameters (viz. back pressure and screw rotation speed) that control the plastication step during which the dispersion process generally begins, were also set up at the lower level. These lower level of injection-molding parameters do not promote the delamination of

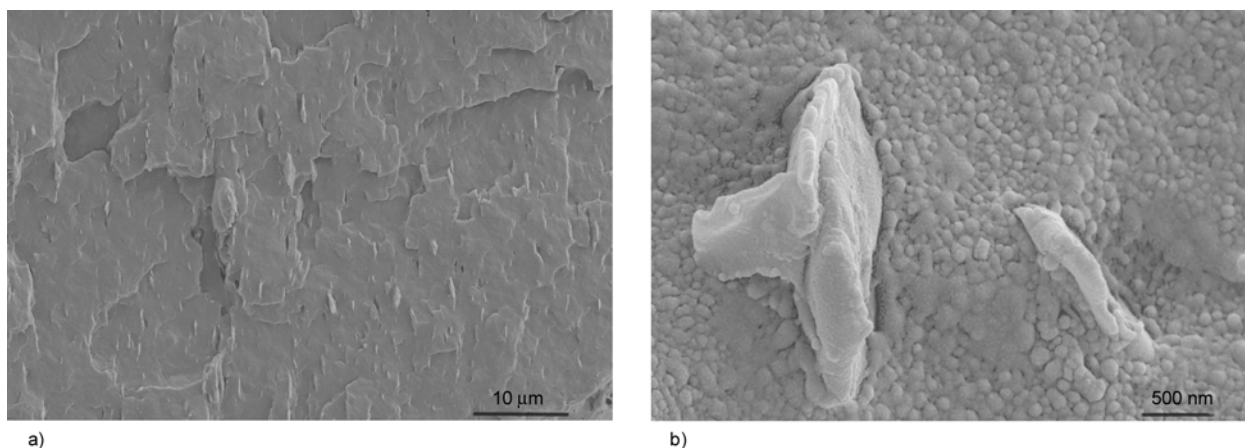


**Figure 4.** SEM images of cryo-fractured surface of NC-L nanocomposite at low (a) and high (b) magnification

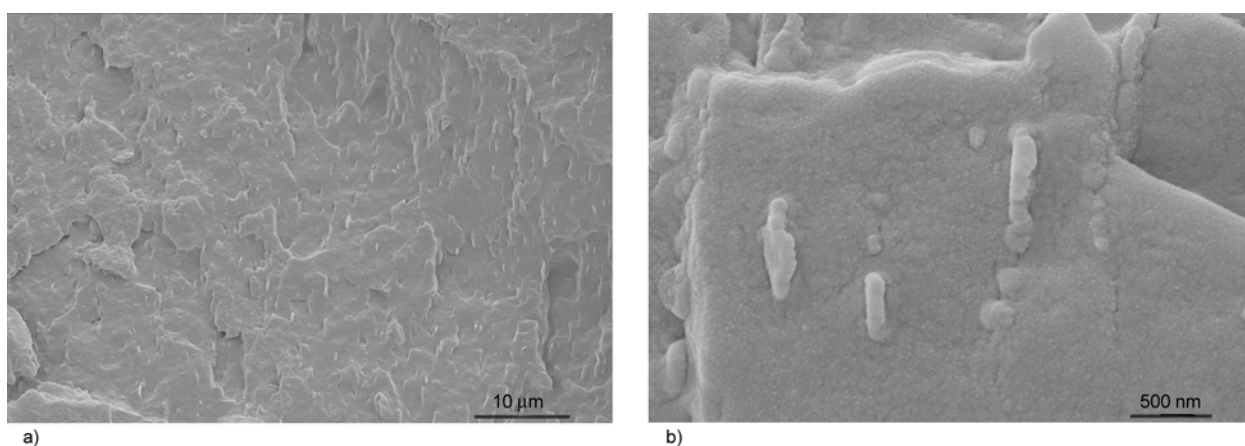


**Figure 5.** SEM images of cryo-fractured surface of NC-H nanocomposite at low (a) and high (b) magnification

the clay tactoids and the homogeneous dispersion of clay platelets. Therefore, the dispersion degree of clay platelets may be lower in NC-L than in NC-H. SEM micrographs (Figure 4b and 5b) also confirm this and hence explain lower storage modulus and complex viscosity values measured for NC-L nanocomposites.

TEM observations (Figure 6 and 7) further provide supporting evidence of the above-mentioned trend. Clay platelets are dispersed as tactoids and the structure of both nanocomposites is intercalated. Few isolated platelets are observed. However, in the case of NC-H nanocomposite some exfoliated clay platelets are visible, even if not in a sufficient number to influence significantly the rheological properties of the nanocomposites. The comparison of NC-H and NC-L nanocomposites TEM observations demonstrates clearly that the dispersion degree is higher in the case of NC-H nanocomposite which presents tactoids of smaller size (length

below 1  $\mu\text{m}$  and width around 200 nm) and thus higher interface area.

However, as attested by the rheological measurements, none of the nanocomposites presents a sufficient dispersion of the layered silicate as the Newtonian plateau remains. Indeed, the increase of  $G'$  and  $|\eta^*|$  is usually attributed to the formation of stable three-dimensional network structures, which might consist of exfoliated clay platelets in larger extent because the percolation network could be built in any polymers regardless of its polarity and molecular weight [38]. Moreover, NC-L and NC-H nanocomposites have low shear thinning behavior compared to results reported elsewhere [39]. Even if the dispersion is improved in the case of NC-H compared to NC-L, no or few exfoliation has occurred and the extent of intercalation is limited compared to the dispersion commonly obtained in the case of PA6 nanocomposites [40–43].

In order to evaluate the effect of the injection-molding induced dispersion of clay, the mechanical

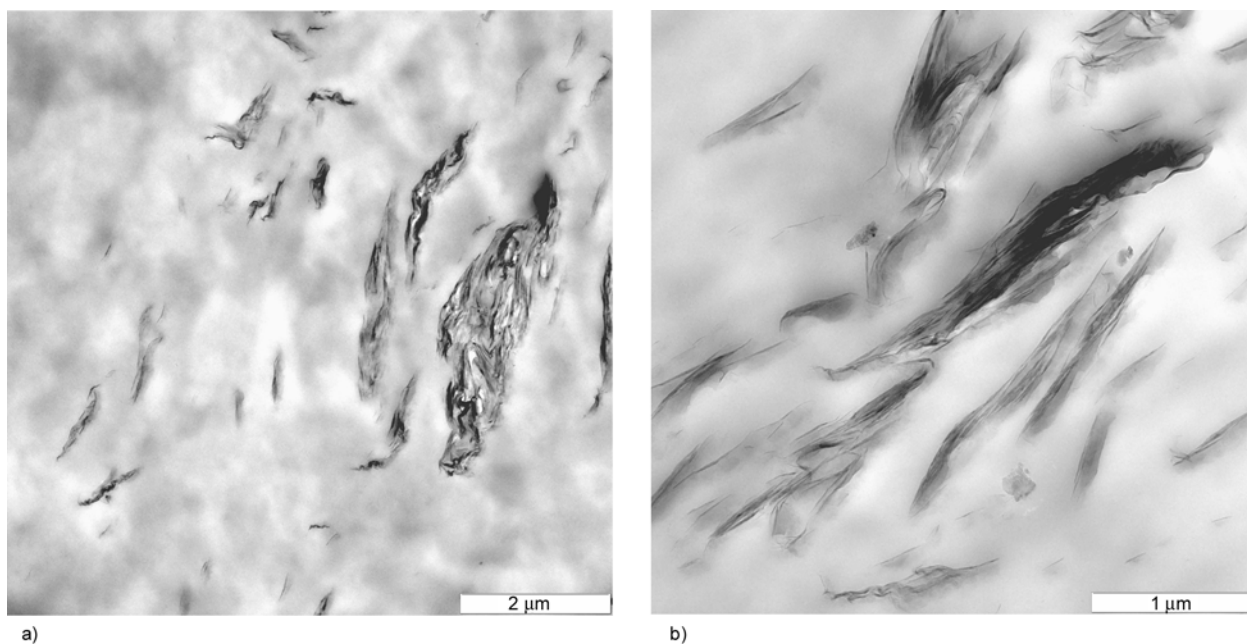


Figure 6. TEM images surface of NC-L nanocomposite at low (a) and high (b) magnification

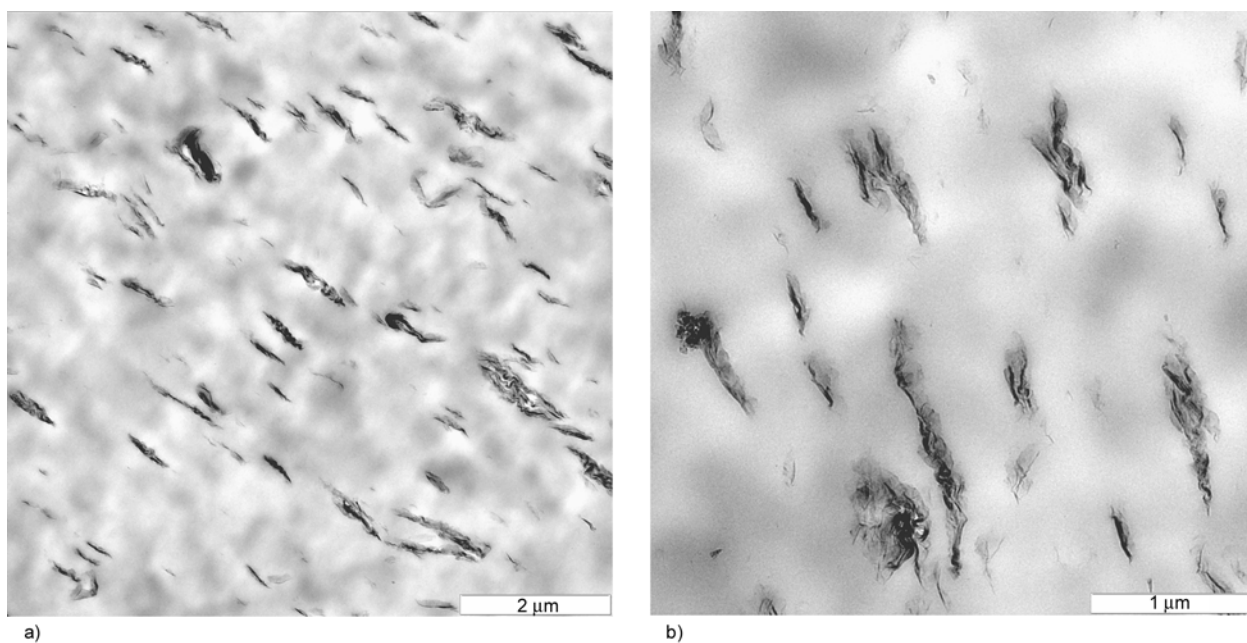


Figure 7. TEM images surface of NC-H nanocomposite at low (a) and high (b) magnification

Table 4. Tensile and Charpy impact properties of PP and PP nanocomposites (average value±standard deviation)

Material	Young modulus [MPa]	Yield stress [MPa]	Tensile el-ongation at break [%]	Stress at break [MPa]	Impact strength – unnotched [kJ/m <sup>2</sup> ]	Impact strength – notched [kJ/m <sup>2</sup> ]
PP-L	1280 ± 20	28.9 ± 0.3	616 ± 15	35.2 ± 0.6	117 ± 8	2.4 ± 0.2
PP-H	1254 ± 23	28.8 ± 0.3	613 ± 12	34.7 ± 0.5	120 ± 9	2.3 ± 0.1
NC-L	1617 ± 54	35.3 ± 0.6	100 ± 22	8.7 ± 6.1	52 ± 4	4.3 ± 0.9
NC-H	1687 ± 45	35.6 ± 0.6	103 ± 23	12.9 ± 5.2	64 ± 8	3.9 ± 0.9

properties of the nanocomposites NC-L and NC-H were measured and compared to neat PP. The values of tensile properties (Young modulus, yield

stress, stress and elongation at break) and Charpy impact strength are reported in Table 4.

Compared to neat PP (PP-L and PP-H), the increase of the Young modulus for NC-L is about 25% whereas the increase for NC-H is slightly higher (30% compared to PP). The dispersion degree does not significantly modify the yield stress. The influence of the clay dispersion degree is much more visible on the stress at break. The higher dispersion degree in the case of NC-H nanocomposite tends to increase significantly (+50%) the stress at break. Whereas the elongation at break is usually expected to be influenced by the dispersion state, the difference between NC-L and NC-H is here negligible, considering the decrease of ductility when the clay platelets are added into the PP matrix and the standard deviations (experimental data dispersion).

A similar trend is observed for the unnotched impact strength (e.g. toughness decrease upon addition of nanoclay into PP). Conversely, in the case of notched impact strength, the nanocomposites NC-L and NC-H have a higher toughness compared to PP. This is due to the fact that notched impact behavior is controlled to a greater extent by factors affecting the propagation of fracture due to stress concentration at the notch tip. The presence of dispersed clay tactoids may restrict the propagation leading to higher toughness as already observed in the case of PP/carbon nanotube nanocomposites [44, 45]. Concerning the impact strength, the toughness of the better dispersed NC-H nanocomposites tends to be higher (+20%) when measured on unnotched samples.

Finally, it may be concluded that the clay dispersion is influenced by the injection molding conditions. This difference of dispersion degree is sufficient to lead to variations in mechanical properties and thus justifies the optimization of the injection molding parameters so as to take the most of these nanocomposites.

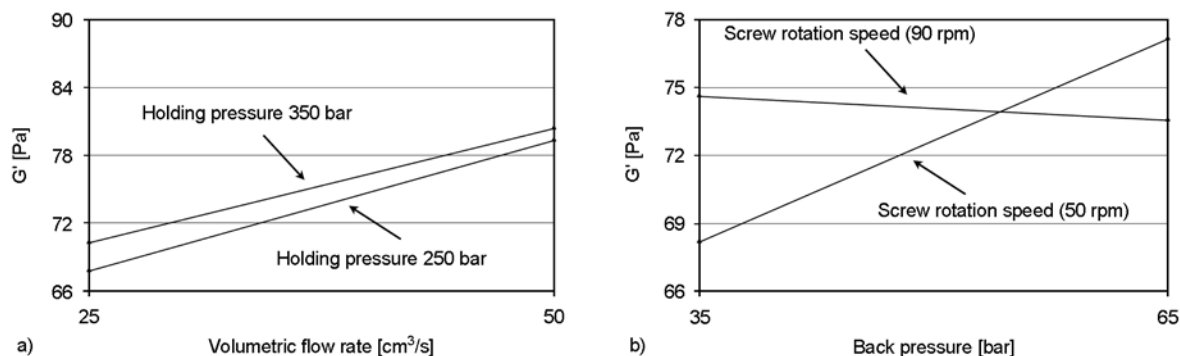


**Figure 9.** Influence of interactions between injection molding parameters on storage modulus  $G'$  of PP/clay nanocomposites

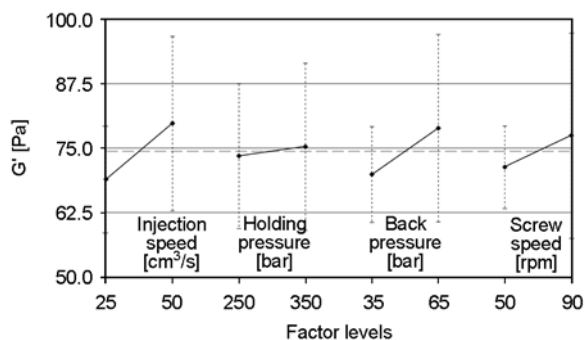


**Figure 8.** Effect of injection molding parameters on storage modulus  $G'$  of PP/Clay nanocomposites – Standard deviations represent data scattering when the considered factor is set-up to its low or high level in the Taguchi DOE

#### 4.2. Optimization of processing parameters

A Taguchi Design Of Experiment (DOE) was used to point out the extent of influence of individual injection molding parameters (also called factors) and their interactions on the nanoclay dispersion [37]. The storage modulus  $G'$  was chosen as output parameter for the Taguchi analysis because of its correlation with the nanoplatelets dispersion as already discussed previously. Figures 8 and 9 respectively present the influence of individual injection molding parameters and the influence of the interactions (Taguchi effect graphs). Figure 10 shows the contributions of the individual parameters and interactions to the storage modulus determined from the DOE.

This Taguchi analysis indicates that injection flow rate and back pressure are the two most important individual injection molding parameters that govern the storage modulus of PP/clay nanocomposites and thus, the nanoplatelets dispersion degree. Among them injection flow rate is the dominant factor. Screw rotation speed has little effect. Holding pressure does not show any effect. Therefore the opti-



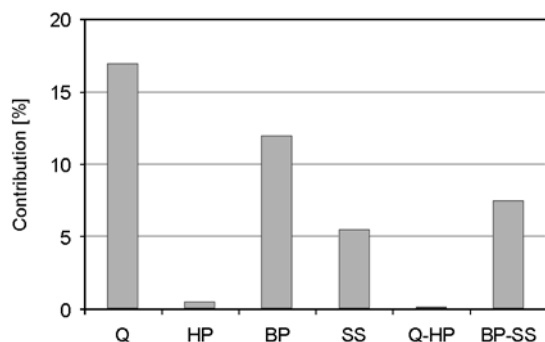


**Figure 10.** Contribution of individual factors and interactions between factors to the storage modulus ( $G'$ ) variations of PP/clay nanocomposites, from the Taguchi DOE analysis

imum injection molding condition for PP nanocomposites leading to the higher storage modulus should have higher injection flow rate, higher back pressure and higher screw rotation speed. The storage modulus data reported in Table 5 confirm this trend. A reduction in holding pressure (NC-3) does not affect the storage modulus significantly compared to NC-H. However, the reduction in any of other three injection molding parameters lowers the storage modulus compared to NC-H, although the extent of decrement depends on the considered injection molding parameter. This set of optimum conditions leading to the highest storage modulus was logically expected because the dispersion of clay layers begins at the plastication step, which

**Table 5.** Experimental data obtained by dynamic rheological measurements – Storage modulus ( $G'$ ) and complex viscosity ( $|\eta^*|$ ) of PP/clay nanocomposites at 0.1 rad/s

Material	$G'$ [Pa]	Complex viscosity, $ \eta^* $ [Pa·s]
NC-1 (NC-H)	107	5270
NC-2	74	4259
NC-3	104	5096
NC-4	79	4385
NC-5	76	4289
NC-6	59	3170
NC-7	73	3657
NC-8	74	3576
NC-9	59	3241
NC-10	62	3314
NC-11	58	3203
NC-12	63	3379
NC-13	80	4409
NC-14	86	4520
NC-15	66	3359
NC-16 (NC-L)	71	3620

involves parameters such as back pressure and screw rotation speed [46]. Generally a higher plastication effect would result in a better distribution and/or dispersion of clay layers. The increase of shearing force due to the high screw rotation speed causes a better dispersion of clay layers whereas the high back pressure further promotes the dispersion and favors the distribution of the clay domains by providing higher residence time in the barrel. Taguchi analysis shows that the back pressure displays a higher contribution (more than twice) as compared to the screw rotation speed. It tends to prove that, considering the plastication step, the optimization of the nanoclay dispersion requires the increase of the residence time more than the increase of shearing. After the plastication step, the injection step is crucial considering that the injection flow rate is the most important parameter and brings a huge change in the storage modulus values (comparison of NC-H and NC-2). The very high shearing forces induced during the injection step may promote the final delamination of the clay tactoids homogeneously distributed during the plastication step.

The interactions between injection flow rate and holding pressure (Q-HP), and between the back pressure and screw rotation speed (BP-SS) were also considered (Figure 9) The interaction between the screw rotation speed and the back pressure has a significant influence on the storage modulus when compared with the contribution of the corresponding factors. Also, the interaction between holding pressure and injection flow rate does not show any effect on the storage modulus. The reduction in both the back pressure and screw rotation speed results in a drastic change in  $G'$  value of NC-H (comparison of NC-H and NC-14) from 107 to 59 Pa, which is the lowest among all nanocomposites. The combined effect of back pressure and screw rotation speed on dispersion is not surprising as these parameters are intimately correlated to the plastication step and promote a longer residence time [46].

Based on these results it can be concluded that the optimization of injection molding parameters could be done as follows. Increasing the shear using high injection flow rate and increasing the residence time by improving the plastication step (high screw rotation speed and mainly high back pressure) result in higher dispersion degree and thus, better

mechanical properties. This is confirmed by rheological measurements as the better dispersion (highest  $G'$ ) is obtained for NC-1 and NC-3, the two samples having these parameters at high level (i.e.  $Q = 50 \text{ cm}^3/\text{s}$ , BP = 65 bars and SS = 90 rpm).

## 5. Conclusions

Injection molding parameters influence the dispersion of clay in PP matrix as attested by the modification of dynamic rheological properties of masterbatch-based melt-mixed PP/clay nanocomposites. Nanocomposites injection-molded at higher back pressure, screw rotational speed, injection flow rate and holding pressure display higher storage modulus and complex viscosity compared to those manufactured with process parameters set-up at lower level. Such improvement achieved with more severe injection molding conditions was attributed to optimized dispersion during injection molding.

The effect of the dispersion degree of the nanoclay on mechanical properties was evaluated. The Young modulus, the Young modulus and the unnotched Charpy impact strength were improved when more severe injection molding parameters were used. Based on a Taguchi analysis, the influence of the individual injection molding parameters and of their interactions on the dispersion was investigated. The injection flow rate and the back pressure are the most influent parameters because of higher shear and longer residence time respectively. The interaction between the back pressure and the screw rotation speed also has a significant influence.

Dilution of highly concentrated PP/clay masterbatches in neat PP is a very promising way to produce polymer nanocomposites injection-molded products in industrially viable conditions. However, the injection molding machine set-up has to take into account the specificity of the polymer nanocomposites. In particular, the dispersion of the nanoplatelets in the final part is a critical issue that requires a careful optimization of the injection molding parameters so as to obtain the expected properties.

## References

[1] Utracki L. A.: Clay-containing polymeric nanocomposites. Rapra Technology, Shawbury (2004).  
 [2] Gupta B., Lacrampe M-F., Krawczak P.: Polyamide-6/clay nanocomposites: A critical review. *Polymers and Polymer Composites*, **14**, 13–38 (2006).

[3] Aloui M., Soulestin J., Lacrampe M-F., Krawczak P., Rousseaux D., Marchand-Brynaert J., Devaux J., Quiévy N., Sclavons M.: A new elaboration concept of polypropylene/unmodified Montmorillonite nanocomposites by reactive extrusion based on direct injection of polypropylene aqueous suspensions. *Polymer Engineering and Science*, **49**, 2276–2285 (2009).  
 DOI: [10.1002/pen.21474](https://doi.org/10.1002/pen.21474)  
 [4] Wang Z. M., Nakajima H., Manias E., Chung T. C.: Exfoliated PP/clay nanocomposites using ammonium-terminated PP as the organic modification for montmorillonite. *Macromolecules*, **36**, 8919–8922 (2003).  
 DOI: [10.1021/ma0352911](https://doi.org/10.1021/ma0352911)  
 [5] Xu L., Nakajima H., Manias E., Krishnamoorti R.: Tailored nanocomposites of polypropylene with layered silicates. *Macromolecules*, **42**, 3795–3803 (2009).  
 DOI: [10.1021/ma9002853](https://doi.org/10.1021/ma9002853)  
 [6] Liao B., Song M., Liang H., Pang Y.: Polymer-layered silicate nanocomposites. 1. A study of poly(ethylene oxide)/Na<sup>+</sup>-montmorillonite nanocomposites as polyelectrolytes and polyethylene-block-poly(ethylene glycol) copolymer/Na<sup>+</sup>-montmorillonite nanocomposites as fillers for reinforcement of polyethylene. *Polymer*, **42**, 10007–10011 (2001).  
 DOI: [10.1016/S0032-3861\(01\)00563-8](https://doi.org/10.1016/S0032-3861(01)00563-8)  
 [7] Reichert P., Hoffmann B., Bock T., Thomann R., Mülhaupt R., Friedrich C.: Morphological stability of poly(propylene) nanocomposites. *Macromolecular Rapid Communications*, **22**, 519–523 (2001).  
 DOI: [10.1002/1521-3927\(20010401\)22:7<519::AID-MARC519>3.0.CO;2-W](https://doi.org/10.1002/1521-3927(20010401)22:7<519::AID-MARC519>3.0.CO;2-W)  
 [8] Gagali G., Ramesh C., Lele A.: A rheological study on the kinetics of hybrid formation in polypropylene nanocomposites. *Macromolecules*, **34**, 852–858 (2001).  
 DOI: [10.1021/ma000565f](https://doi.org/10.1021/ma000565f)  
 [9] Solomon M. J., Almusallam Q. S., Seefeldt K. F., Somwangthanaroj A., Varadan P.: Rheology of polypropylene/clay hybrid materials. *Macromolecules*, **34**, 1864–1872 (2001).  
 DOI: [10.1021/ma001122e](https://doi.org/10.1021/ma001122e)  
 [10] García-López D., Picazo O., Merino J. C., Pastor J. M.: Polypropylene–clay nanocomposites: Effect of compatibilizing agents on clay dispersion. *European Polymer Journal*, **39**, 945–950 (2003).  
 DOI: [10.1016/S0014-3057\(02\)00333-6](https://doi.org/10.1016/S0014-3057(02)00333-6)  
 [11] Jian L., Zhou C., Gang W., Wei Y., Ying T., Qing L.: Preparation and linear rheological behavior of polypropylene/MMT nanocomposites. *Polymer Composites*, **24**, 323–331 (2003).  
 DOI: [10.1002/pc.10032](https://doi.org/10.1002/pc.10032)  
 [12] Li J., Zhou C., Wang G., Zhao D.: Study on rheological behavior of polypropylene/clay nanocomposites. *Journal of Applied Polymer Science*, **89**, 3609–3617 (2003).  
 DOI: [10.1002/app.12643](https://doi.org/10.1002/app.12643)

- [13] Gu S-Y., Ren J., Wang Q-F.: Rheology of poly(propylene)/clay nanocomposites. *Journal of Applied Polymer Science*, **91**, 2427–2434 (2004).  
DOI: [10.1002/app.13403](https://doi.org/10.1002/app.13403)
- [14] Treece M. A., Oberhauser J. P.: Soft glassy dynamics in polypropylene–clay nanocomposites. *Macromolecules*, **40**, 571–582 (2007).  
DOI: [10.1021/ma0612374](https://doi.org/10.1021/ma0612374)
- [15] Manias E., Touny A., Wu L., Strawhecker K., Lu B., Chung T. C.: Polypropylene/montmorillonite nanocomposites. Review of the synthetic routes and materials properties. *Chemistry of Materials*, **13**, 3516–3523 (2001).  
DOI: [10.1021/cm0110627](https://doi.org/10.1021/cm0110627)
- [16] Rousseaux D. D. J., Sallem-Idrissi N., Baudouin A., Devaux J., Godard P., Marchand-Brynaert J., Scavons M.: Water-assisted extrusion of polypropylene/clay nanocomposites: A comprehensive study. *Polymer*, **52**, 443–451 (2011).  
DOI: [10.1016/j.polymer.2010.11.027](https://doi.org/10.1016/j.polymer.2010.11.027)
- [17] Trotignon J-P., Verdu J.: Skin-core structure–fatigue behavior relationships for injection-molded parts of polypropylene. I. Influence of molecular weight and injection conditions on the morphology. *Journal of Applied Polymer Science*, **34**, 1–18 (1987).  
DOI: [10.1002/app.1987.070340101](https://doi.org/10.1002/app.1987.070340101)
- [18] Čermák R., Obadal M., Ponížil P., Polášková M., Stoklasa K., Lengálová A.: Injection-moulded  $\alpha$ - and  $\beta$ -polypropylenes: I. Structure vs. processing parameters. *European Polymer Journal*, **41**, 1838–1845 (2005).  
DOI: [10.1016/j.eurpolymj.2005.02.020](https://doi.org/10.1016/j.eurpolymj.2005.02.020)
- [19] LaFranché E., Brassart G., Krawczak P.: Processing-induced morphology: Its relationship with tensile-impact behaviour in injection-moulded polypropylene. *Polymers and Polymer Composites*, **14**, 563–576 (2006).
- [20] Médéric P., Razafinimaro T., Aubry T., Moan M., Klopffer M-H.: Rheological and structural investigation of layered silicate nanocomposites based on polyamide or polyethylene: Influence of processing conditions and volume fraction effects. *Macromolecular Symposia*, **221**, 75–84 (2005).  
DOI: [10.1002/masy.200550308](https://doi.org/10.1002/masy.200550308)
- [21] Peltola P., Välipakka E., Vuorinen J., Syrjälä S., Hanhi K.: Effect of rotational speed of twin screw extruder on the microstructure and rheological and mechanical properties of nanoclay-reinforced polypropylene nanocomposites. *Polymer Engineering and Science*, **46**, 995–1000 (2006).  
DOI: [10.1002/pen.20586](https://doi.org/10.1002/pen.20586)
- [22] Lertwimolnun W., Vergnes B.: Influence of compatibilizer and processing conditions on the dispersion of nanoclay in a polypropylene matrix. *Polymer*, **46**, 3462–3471 (2005).  
DOI: [10.1016/j.polymer.2005.02.018](https://doi.org/10.1016/j.polymer.2005.02.018)
- [23] Modesti M., Lorenzetti A., Bon D., Besco S.: Effect of processing conditions on morphology and mechanical properties of compatibilized polypropylene nanocomposites. *Polymer*, **46**, 10237–10245 (2005).  
DOI: [10.1016/j.polymer.2005.08.035](https://doi.org/10.1016/j.polymer.2005.08.035)
- [24] Kracalik M., Laske S., Gschweiltl M., Friesenbichler W., Langecker G. R.: Advanced compounding: Extrusion of polypropylene nanocomposites using the melt pump. *Journal of Applied Polymer Science*, **113**, 1422–1428 (2009).  
DOI: [10.1002/app.29888](https://doi.org/10.1002/app.29888)
- [25] Treece M. A., Zhang W., Moffitt R. D., Oberhauser J. P.: Twin-screw extrusion of polypropylene-clay nanocomposites: Influence of masterbatch processing, screw rotation mode, and sequence. *Polymer Engineering and Science*, **47**, 898–911 (2007).  
DOI: [10.1002/pen.20774](https://doi.org/10.1002/pen.20774)
- [26] Li Y-C., Chen G-H.: HDPE/expanded graphite nanocomposites prepared via masterbatch process. *Polymer Engineering and Science*, **47**, 882–888 (2007).  
DOI: [10.1002/pen.20772](https://doi.org/10.1002/pen.20772)
- [27] Pötschke P., Bhattacharyya A. R., Alig I., Dudkin S. M., Leonhardt A., Täschner C., Ritschel M., Roth S., Hornbostel B., Cech J.: Dispersion of carbon nanotubes into thermoplastic polymers using melt mixing. in ‘Electronic properties of synthetic nanostructures: XVIII international winterschool/euroconference on electronic properties of novel materials’ (eds.: Kuzmany H., Fink J., Mehring M., Roth S.) American Institute of Physics, Washington 478–482 (2004).
- [28] Shah R. K., Paul D. R.: Nylon 6 nanocomposites prepared by a melt mixing masterbatch process. *Polymer*, **45**, 2991–3000 (2004).  
DOI: [10.1016/j.polymer.2004.02.058](https://doi.org/10.1016/j.polymer.2004.02.058)
- [29] Yilmazer U., Ozden G.: Polystyrene–organoclay nanocomposites prepared by melt intercalation, in situ, and masterbatch methods. *Polymer Composites*, **27**, 249–255 (2006).  
DOI: [10.1002/pc.20191](https://doi.org/10.1002/pc.20191)
- [30] Dorigato A., Pegoretti A., Penati A.: Linear low-density polyethylene/silica micro- and nanocomposites: Dynamic rheological measurements and modelling. *Express Polymer Letters*, **4**, 115–129 (2010).  
DOI: [10.3144/expresspolymlett.2010.16](https://doi.org/10.3144/expresspolymlett.2010.16)
- [31] Sarvestani A. S.: Modeling the solid-like behavior of entangled polymer nanocomposites at low frequency regimes. *European Polymer Journal*, **44**, 263–269 (2008).  
DOI: [10.1016/j.eurpolymj.2007.11.023](https://doi.org/10.1016/j.eurpolymj.2007.11.023)
- [32] Le Meins J-F., Moldenaers P., Mewis J.: Suspensions in polymer melts. 1. Effect of particle size on the shear flow behavior. *Industrial and Engineering Chemistry Research*, **41**, 6297–6304 (2002).  
DOI: [10.1021/ie020117r](https://doi.org/10.1021/ie020117r)
- [33] Osman M. A., Atallah A.: Interparticle and particle–matrix interactions in polyethylene reinforcement and viscoelasticity. *Polymer*, **46**, 9476–9488 (2005).  
DOI: [10.1016/j.polymer.2005.07.030](https://doi.org/10.1016/j.polymer.2005.07.030)

- [34] Hoffmann B., Kressler J., Stöpplemann G., Friedrich C., Kim G-M.: Rheology of nanocomposites based on layered silicates and polyamide-12. *Colloid and Polymer Science*, **278**, 629–636 (2000).  
DOI: [10.1007/s003960000294](https://doi.org/10.1007/s003960000294)
- [35] Chow W. S., Mohd Ishak Z. A., Karger-Kocsis J.: Morphological and rheological properties of polyamide 6/poly(propylene)/organoclay nanocomposites. *Macromolecular Materials and Engineering*, **290**, 122–127 (2005).  
DOI: [10.1002/mame.200400269](https://doi.org/10.1002/mame.200400269)
- [36] Wang K., Zhao P., Yang H., Liang S., Zhang Q., Du R., Fu Q., Yu Z., Chen E.: Unique clay orientation in the injection-molded bar of isotactic polypropylene/clay nanocomposite. *Polymer*, **47**, 7103–7110 (2006).  
DOI: [10.1016/j.polymer.2006.08.022](https://doi.org/10.1016/j.polymer.2006.08.022)
- [37] Taguchi G., Konishi S., Wu Y.: *Quality engineering series, Vol. 1, Taguchi methods, research and development*. ASI, Dearborn (1992).
- [38] Wang K., Liang S., Zhao P., Qu C., Tan H., Du R., Zhang Q., Fu Q.: Correlation of rheology–orientation–tensile property in isotactic polypropylene/organoclay nanocomposites. *Acta Materialia*, **55**, 3143–3154 (2007).  
DOI: [10.1016/j.actamat.2007.01.020](https://doi.org/10.1016/j.actamat.2007.01.020)
- [39] Ray S. S.: Rheology of polymer/layered silicate nanocomposites. *Journal of Industrial and Engineering Chemistry*, **12**, 811–842 (2006).
- [40] Zhao J., Morgan A. B., Harris J. D.: Rheological characterization of polystyrene–clay nanocomposites to compare the degree of exfoliation and dispersion. *Polymer*, **46**, 8641–8660 (2005).  
DOI: [10.1016/j.polymer.2005.04.038](https://doi.org/10.1016/j.polymer.2005.04.038)
- [41] Samyn F., Bourbigot S., Jama C., Bellayer S., Nazare S., Hull R., Castrovinci A., Fina A., Camino G.: Crossed characterisation of polymer-layered silicate (PLS) nanocomposite morphology: TEM, X-ray diffraction, rheology and solid-state nuclear magnetic resonance measurements. *European Polymer Journal*, **44**, 1642–1653 (2008).  
DOI: [10.1016/j.eurpolymj.2008.03.021](https://doi.org/10.1016/j.eurpolymj.2008.03.021)
- [42] Soulestin J., Rashmi B. J., Bourbigot S., Lacrampe M. F., Krawczak P.: Mechanical and optical properties of polyamide 6/clay nanocomposite cast-films: Influence of the exfoliation degree. *Macromolecular Materials and Engineering*, in press (2011).  
DOI: [10.1002/mame.201100202](https://doi.org/10.1002/mame.201100202)
- [43] Touchaleaume F., Soulestin J., Scavons M., Devaux J., Lacrampe M. F., Krawczak P.: One-step water-assisted melt-compounding of polyamide 6/pristine clay nanocomposites: An efficient way to prevent matrix degradation. *Polymer Degradation and Stability*, **96**, 1890–1900 (2011).  
DOI: [10.1016/j.polymdegradstab.2011.07.005](https://doi.org/10.1016/j.polymdegradstab.2011.07.005)
- [44] Prashantha K., Soulestin J., Lacrampe M. F., Claes M., Dupin G., Krawczak P.: Multi-walled carbon nanotube filled polypropylene nanocomposites based on masterbatch route: Improvement of dispersion and mechanical properties through PP-g-MA addition. *Express Polymer Letters*, **2**, 735–745 (2008).  
DOI: [10.3144/expresspolymlett.2008.87](https://doi.org/10.3144/expresspolymlett.2008.87)
- [45] Prashantha K., Soulestin J., Lacrampe M. F., Krawczak P., Dupin G., Claes M.: Masterbatch-based multi-walled carbon nanotube filled polypropylene nanocomposites: Assessment of rheological and mechanical properties. *Composites Science and Technology*, **69**, 1756–1763 (2009).  
DOI: [10.1016/j.compscitech.2008.10.005](https://doi.org/10.1016/j.compscitech.2008.10.005)
- [46] Rosato D. V., Rosato M. G.: *Injection molding handbook*. Kluwer, Norwell (2000).